

**Acoustic properties of double-porosity granular polymers**A. Alevizaki,<sup>1,2,\*</sup> R. Sainidou,<sup>1</sup> P. Rembert,<sup>1</sup> B. Morvan,<sup>1</sup> and N. Stefanou<sup>2</sup><sup>1</sup>*Normandie Univ, UNIHAVRE, Laboratoire Ondes et Milieux Complexes, UMR CNRS 6294, 75 rue Bellot, 76600 Le Havre, France*<sup>2</sup>*Department of Solid State Physics, National and Kapodistrian University of Athens, University Campus, GR-157 84 Athens, Greece*

(Received 14 March 2017; revised manuscript received 18 May 2017; published 14 June 2017)

Using an extension of the full elastodynamic layer-multiple-scattering method to structures of fluid-saturated poroelastic spherical bodies, a comprehensive theoretical study of the acoustic response of double-porosity submerged liquid-saturated granular polymeric materials of specific morphology consisting of touching porous polymer spheres arranged in a fcc lattice, beyond the long-wavelength effective-medium description, is presented. Calculated transmission and absorption spectra of finite slabs of these materials are analyzed by reference to the acoustic modes of the constituent porous spherical grains as well as to relevant dispersion diagrams of corresponding infinite crystals, and a consistent interpretation of the results is provided. In particular, it is shown that resonant modes with very long lifetime, localized in the spheres in the form of slow longitudinal waves, which are peculiar to poroelastic materials, are formed when the viscous length is much shorter than the radius of the inner pores of the spheres. These modes, which can be easily tuned in frequency by adjusting the intrinsic porosity of the spheres, induce some remarkable features in the acoustic behavior of these double-porosity materials, such as narrow dispersionless absorption bands and directional transmission gaps.

DOI: [10.1103/PhysRevB.95.214306](https://doi.org/10.1103/PhysRevB.95.214306)**I. INTRODUCTION**

Hierarchically porous materials, which by definition contain a network of interconnected pores with sizes at different length scales, is a promising class of natural or synthetic structures offering a large spectrum of functionalities in various application domains [1] and also of interest for a fundamental theoretical understanding. In particular, hierarchically porous polymeric materials synthesized by various methods have attracted increasing interest in recent years [2–8] because of their potential applications in different fields, including catalysis, separation technology, gas storage, and bioengineering. However, the acoustic properties of such materials did not receive considerable attention so far.

Biot's theory [9,10], though it is perfectly appropriate for an effective description of poroelastic media with a more or less uniform pore distribution, i.e., a single-porosity structure, fails to describe hierarchically porous materials with pore sizes at different length scales. A variety of homogenization methods, beyond Biot's theory, have been developed for a macroscopic description of such media and, in particular, of double-porosity deformable media characterized by two interconnected networks of fluid-saturated pores of very different sizes that exhibit very different permeabilities (see, e.g., Ref. [11] and references therein). The validity of these methods has been examined in a number of theoretical and experimental works. Franklin *et al.* [12] studied acoustic wave propagation in a water-saturated double-porosity medium, consisting of a random array of parallel identical cylindrical holes of infinite length, perpendicular to the direction of propagation, in an otherwise single-porosity material described by Biot's theory, by means of two-dimensional (2D) multiple-scattering calculations in the long-wavelength approximation and compared with the results of appropriate effective-medium descriptions. Acoustic wave propagation has also been investigated in

periodic mixtures of two different porous media which occupy two disjoint subdomains at the mesoscopic scale, in one and two dimensions, through numerical simulations by the finite-elements method in conjunction with relevant homogenization models in both high- and low-permeability-contrast regimes [13]. The predictions of analytical and semianalytical effective-medium methods for the acoustic properties of double-porosity granular materials have been experimentally confirmed on expanded perlite and activated carbon, revealing stronger low-frequency sound absorption at reduced weight (porous grains) compared to a solid-grain granular material with similar mesoscopic characteristics [14]. Moreover, the observed macroscopic acoustic behavior of mineral double-porosity foams was also explained by relevant effective-medium modeling [15]. However, all local homogenization methods break down if the size of the representative elementary volume, which defines the scale of heterogeneity, is not much smaller than the wavelength [11].

In the present paper we shall be concerned with the acoustic properties of water-saturated double-porosity polymeric materials with a specific morphology, formed by close-packed poroelastic spheres arranged in a face-centered cubic (fcc) lattice. Our study will be restricted to wavelengths much longer than the radius of the sphere's pores and the distance between them, so that Biot's theory is applicable at this level [9,10], but not long enough compared to the interstitial void structure, thus requiring a rigorous description of acoustic multiple scattering between the spheres beyond a homogenization theory. Thermal losses are omitted in our study since the saturating fluid is a liquid and thus, in contrast to the case of a gas, the characteristic thermal skin depth is much shorter than the corresponding viscous length, while viscosity is taken into account only in the fluid that fills the pores of the spheres [16]. It is worth noting that, though the open pores and the solid skeletal frame of the individual spheres, as well as the interstitial voids, have the percolating network topology, this is not the case for the solid (polymer) material throughout the structure because neighboring spheres are touching but

\*athina.alevizaki@univ-lehavre.fr

not consolidated. Therefore, while according to Biot's theory, transverse, fast, and slow longitudinal waves subsist inside the spheres, only the common longitudinal waves in the fluid matrix (water) constitute propagating modes of the acoustic field in the double-porosity medium under consideration [17].

The paper is structured as follows. In Sec. II we describe in a detailed but concise manner the method of calculation, namely our layer-multiple-scattering method [18,19], which we recently extended to include porous fluid-saturated scatterers [20], by adapting it in the case of interest, i.e., for acoustic scattering. Next, we present, in Sec. III, its application on a double-porosity polymer close-packed crystal, accompanying the numerical calculations by a thorough physical analysis, and we draw the major conclusions in Sec. IV.

## II. METHOD OF CALCULATION

The displacement field associated with a time-harmonic, monochromatic acoustic wave, of angular frequency  $\omega$ , has the form  $\mathbf{U}(\mathbf{r}, t) = \text{Re}[\mathbf{U}(\mathbf{r}) \exp(-i\omega t)]$ . For a plane wave of wave vector  $\mathbf{q}_h$ , propagating in a homogeneous inviscid fluid medium characterized by mass density  $\rho_h$  and bulk modulus  $K_h$  (we denote it by an index zero), we have

$$\mathbf{U}_0(\mathbf{r}) = \hat{\mathbf{q}}_h U_0 \exp(i\mathbf{q}_h \cdot \mathbf{r}), \quad (1)$$

where  $q_h = \omega \sqrt{\rho_h/K_h}$  is the wave number and  $U_0$  is the field amplitude. Using the mathematical identities:  $\mathbf{q}_h \exp(i\mathbf{q}_h \cdot \mathbf{r}) = -i \nabla \exp(i\mathbf{q}_h \cdot \mathbf{r})$  and  $\exp(i\mathbf{q}_h \cdot \mathbf{r}) = 4\pi \sum_{\ell m} i^\ell j_\ell(q_h r) Y_{\ell m}(\hat{\mathbf{r}}) Y_{\ell m}^*(\hat{\mathbf{q}}_h)$ , where  $j_\ell$  are the spherical Bessel functions and  $Y_{\ell m}$  the spherical harmonics [21], the plane wave of Eq. (1) can be readily expanded into vector spherical waves as follows:

$$\mathbf{U}_0(\mathbf{r}) = \sum_{\ell m} a_{L\ell m}^0 \frac{1}{q_h} \nabla [j_\ell(q_h r) Y_{\ell m}(\hat{\mathbf{r}})], \quad (2)$$

where the amplitudes of the partial waves are given by  $a_{L\ell m}^0 = 4\pi i^{\ell+1} (-1)^{m+1} Y_{\ell-m}(\hat{\mathbf{q}}_h) U_0$ .

When the above plane wave is incident on a submerged fluid-saturated poroelastic sphere of radius  $S$ , centered at the origin of coordinates, it is scattered by it, so that the total displacement field outside the sphere consists of the incident wave and a scattered wave, which can also be expanded into longitudinal spherical waves as follows:

$$\mathbf{U}_{sc}(\mathbf{r}) = \sum_{\ell m} a_{L\ell m}^+ \frac{1}{q_h} \nabla [h_\ell^+(q_h r) Y_{\ell m}(\hat{\mathbf{r}})], \quad (3)$$

where  $h_\ell^+$  are the spherical Hankel functions appropriate for outgoing spherical waves:  $h_\ell^+ \simeq (-i)^\ell \exp(ix)/(ix)$  as  $x \rightarrow \infty$  [21]. The amplitudes of the scattered spherical waves,  $a_{L\ell m}^+$ , are linearly related to their counterparts  $a_{L\ell m}^0$  as follows:

$$a_{L\ell m}^+ = \sum_{\ell' m'} T_{L\ell m; L\ell' m'} a_{L\ell' m'}^0, \quad (4)$$

where  $T_{L\ell m; L\ell' m'}$ , the elements of the so-called scattering  $T$  matrix, are obtained by applying the appropriate boundary conditions at the surface of the scatterer. Explicit equations for the calculation of  $T_{L\ell m; L\ell' m'}$  in the case of a submerged fluid-saturated poroelastic sphere have been derived elsewhere [20]. We note that, in our case, as implied by spherical

symmetry, the  $T$  matrix is diagonal and does not depend on  $m$ , i.e.,  $T_{L\ell m; L\ell' m'} = T_{LL; \ell} \delta_{\ell\ell'} \delta_{mm'}$ .

With the help of the  $T$  matrix one can directly calculate the change in the number of states of the acoustic field, up to an angular frequency  $\omega$ , induced by a single poroelastic sphere in an infinite fluid host medium from [22]

$$\Delta N(\omega) = \frac{1}{\pi} \sum_{\ell} (2\ell + 1) \text{Im} \ln[1 + T_{LL; \ell}(\omega)]. \quad (5)$$

Of more interest is the corresponding change in the density of states induced by the sphere and given by

$$\Delta n(\omega) = \frac{d\Delta N(\omega)}{d\omega}. \quad (6)$$

On the other hand, the total scattering and extinction cross sections of the sphere, normalized to the geometric cross section  $\pi S^2$ , can also be expressed in terms of the  $T$  matrix as follows [23]:

$$\sigma_{sc}(\omega) = \frac{4}{(q_h S)^2} \sum_{\ell} (2\ell + 1) |T_{LL; \ell}(\omega)|^2 \quad (7)$$

and

$$\sigma_{ext}(\omega) = -\frac{4}{(q_h S)^2} \sum_{\ell} (2\ell + 1) \text{Re}[T_{LL; \ell}(\omega)], \quad (8)$$

respectively, while the corresponding absorption cross section is given by  $\sigma_{abs} = \sigma_{ext} - \sigma_{sc}$ .

We now consider a plane of nonoverlapping submerged water-saturated poroelastic spheres, at  $z = 0$ , which are centered on the sites  $\mathbf{R}_n$  of a given 2D lattice. Let the plane wave, described by Eq. (1), be incident on this layer. Because of the 2D periodicity of the structure under consideration, we write the component of the wave vector of the incident wave parallel to the plane,  $\mathbf{q}_{\parallel}$ , as  $\mathbf{q}_{\parallel} = \mathbf{k}_{\parallel} + \mathbf{g}'$ , where  $\mathbf{k}_{\parallel}$ , the reduced wave vector in the surface Brillouin zone (SBZ), is a conserved quantity in the scattering process and  $\mathbf{g}'$  is a certain reciprocal vector of the given lattice. Therefore, the wave vector of the incident wave has the form  $\mathbf{K}_{\mathbf{g}}^{\pm} = \mathbf{k}_{\parallel} + \mathbf{g}' \pm \hat{\mathbf{z}}[q_h^2 - (\mathbf{k}_{\parallel} + \mathbf{g}')^2]^{1/2}$ , where the  $+$  or  $-$  sign refers to incidence from the left ( $z < 0$ ) or from the right ( $z > 0$ ). The corresponding displacement field is written as

$$\mathbf{U}_{in}^{\pm}(\mathbf{r}) = \hat{\mathbf{K}}_{\mathbf{g}}^{\pm} [U_{in}]_{\mathbf{g}}^{\pm} \exp(i\mathbf{K}_{\mathbf{g}}^{\pm} \cdot \mathbf{r}) \quad (9)$$

and the coefficients in the respective spherical wave expansion [see Eq. (2)] are  $a_{L\ell m}^0 = 4\pi i^{\ell+1} (-1)^{m+1} Y_{\ell-m}(\hat{\mathbf{K}}_{\mathbf{g}}^{\pm}) [U_{in}]_{\mathbf{g}}^{\pm}$ .

Because of the 2D periodicity of the array of spheres, the wave scattered by it, when the wave given by Eq. (9) is incident upon it, has the following form:

$$\mathbf{U}_{sc}(\mathbf{r}) = \sum_{\mathbf{R}_n} \exp(i\mathbf{k}_{\parallel} \cdot \mathbf{R}_n) \sum_{\ell m} b_{L\ell m}^+ \frac{1}{q_h} \nabla [h_\ell^+(q_h r_n) Y_{\ell m}(\hat{\mathbf{r}}_n)], \quad (10)$$

where  $\mathbf{r}_n = \mathbf{r} - \mathbf{R}_n$  and the coefficients  $b_{L\ell m}^+$  are obtained by solving the following system of linear equations [18]:

$$\sum_{\ell' m'} (\delta_{\ell\ell'} \delta_{mm'} - T_{LL; \ell} Z_{\ell' m'}^{\ell m}) b_{L\ell' m'}^+ = T_{LL; \ell} a_{L\ell m}^0, \quad (11)$$

with

$$\begin{aligned} Z_{\ell m}^{\ell' m'} &= 4\pi \sum_{\mathbf{R}_n \neq 0} \exp(i\mathbf{k}_{\parallel} \cdot \mathbf{R}_n) \sum_{\ell'' m''} (-1)^{(\ell - \ell' - \ell'')/2} \\ &\times (-1)^{m' + m''} h_{\ell''}^+(q_h R_n) Y_{\ell'' - m''}(-\hat{\mathbf{R}}_n) \\ &\times \int d\hat{\mathbf{r}} Y_{\ell m}(\hat{\mathbf{r}}) Y_{\ell' - m'}(\hat{\mathbf{r}}) Y_{\ell'' m''}(\hat{\mathbf{r}}), \end{aligned} \quad (12)$$

which is a well-known quantity in the theory of low-energy electron diffraction (LEED) with an efficient computer program for its evaluation already available [24]. This program is used in the numerical implementation of our layer-multiple-scattering method [19]. Similar approaches for the calculation of such lattice sums for chains and monolayers have also been recently reported in the literature, discussing in some detail novel numerical aspects [25,26].

Since  $\omega$  and  $\mathbf{k}_{\parallel}$  are conserved quantities in the scattering process, the scattered field, given by Eq. (10), will consist of a series of plane waves with wave vectors,

$$\mathbf{K}_{\mathbf{g}}^{\pm} = \mathbf{k}_{\parallel} + \mathbf{g} \pm \hat{\mathbf{z}} [q_h^2 - (\mathbf{k}_{\parallel} + \mathbf{g})^2]^{1/2}, \quad \forall \mathbf{g}. \quad (13)$$

Indeed, with the help of the mathematical identity

$$\begin{aligned} \sum_{\mathbf{R}_n} \exp(i\mathbf{k}_{\parallel} \cdot \mathbf{R}_n) h_{\ell}^+(q_h r_n) Y_{\ell m}(\hat{\mathbf{r}}_n) \\ = \sum_{\mathbf{g}} \frac{2\pi(-i)^{\ell}}{q_h A_0 K_{\mathbf{g}z}^+} Y_{\ell m}(\hat{\mathbf{K}}_{\mathbf{g}}^s) \exp(i\mathbf{K}_{\mathbf{g}}^s \cdot \mathbf{r}), \end{aligned} \quad (14)$$

where  $A_0$  is the area of the unit cell of the 2D lattice and  $s = +$  or  $-$  corresponds to  $z > 0$  or  $z < 0$ , respectively, it is straightforward to show that

$$\mathbf{U}_{sc}(\mathbf{r}) = \sum_{\mathbf{g}} \hat{\mathbf{K}}_{\mathbf{g}}^s [U_{sc}]_{\mathbf{g}}^s \exp(i\mathbf{K}_{\mathbf{g}}^s \cdot \mathbf{r}), \quad (15)$$

with

$$[U_{sc}]_{\mathbf{g}}^s = \sum_{\ell m} \Delta_{L\ell m}(\mathbf{K}_{\mathbf{g}}^s) b_{L\ell m}^+,$$

where

$$\Delta_{L\ell m}(\mathbf{K}_{\mathbf{g}}^s) = \frac{2\pi(-i)^{\ell-1}}{q_h A_0 K_{\mathbf{g}z}^+} Y_{\ell m}(\hat{\mathbf{K}}_{\mathbf{g}}^s).$$

It is worth noting that, though the scattered field consists, in general, of a number of diffracted beams corresponding to different 2D reciprocal lattice vectors  $\mathbf{g}$ , only beams for which  $K_{\mathbf{g}z}^s$  is real constitute propagating waves. When  $(\mathbf{k}_{\parallel} + \mathbf{g})^2 > q_h^2$  the corresponding wave decays to the right for  $s = +$ , and to the left for  $s = -$ . We also note that  $[U_{sc}]_{\mathbf{g}}^s$  depend on the incident plane wave through the coefficients  $b_{L\ell m}^+$ , which are evaluated from Eqs. (11) for a given plane wave component of wave vector  $\mathbf{K}_{\mathbf{g}}^s$ . For example, when a plane wave given by Eq. (9) is incident on the plane of spheres from the left, the transmitted wave (incident+scattered) on the right of the plane is given by

$$\mathbf{U}_{tr}^+(\mathbf{r}) = \sum_{\mathbf{g}} \hat{\mathbf{K}}_{\mathbf{g}}^+ [U_{tr}]_{\mathbf{g}}^+ \exp(i\mathbf{K}_{\mathbf{g}}^+ \cdot \mathbf{r}), \quad z > 0, \quad (16)$$

with

$$[U_{tr}]_{\mathbf{g}}^+ = [U_{in}]_{\mathbf{g}}^+ \delta_{\mathbf{g}\mathbf{g}'} + [U_{sc}]_{\mathbf{g}}^+ \equiv S_{\mathbf{g}\mathbf{g}'}^{++} [U_{in}]_{\mathbf{g}'}^+,$$

and the reflected wave on the left of the plane by

$$\mathbf{U}_{rf}^-(\mathbf{r}) = \sum_{\mathbf{g}} \hat{\mathbf{K}}_{\mathbf{g}}^- [U_{rf}]_{\mathbf{g}}^- \exp(i\mathbf{K}_{\mathbf{g}}^- \cdot \mathbf{r}), \quad z < 0, \quad (17)$$

with

$$[U_{rf}]_{\mathbf{g}}^- = [U_{sc}]_{\mathbf{g}}^- \equiv S_{\mathbf{g}\mathbf{g}'}^{-+} [U_{in}]_{\mathbf{g}'}^+.$$

Similarly we can define the transmission matrix elements  $S_{\mathbf{g}\mathbf{g}'}^{-}$  and the reflection matrix elements  $S_{\mathbf{g}\mathbf{g}'}^{+}$  for a plane wave incident on the plane of spheres from the right. Using Eq. (15) we obtain

$$S_{\mathbf{g}\mathbf{g}'}^{ss'} = \delta_{ss'} \delta_{\mathbf{g}\mathbf{g}'} + \sum_{\ell m} \Delta_{L\ell m}(\mathbf{K}_{\mathbf{g}}^s) b_{L\ell m}^+(\mathbf{K}_{\mathbf{g}'}^{s'}) ([U_{in}]_{\mathbf{g}'}^{s'})^{-1}, \quad (18)$$

where we explicitly denoted the dependence of  $b_{L\ell m}^+$  on  $\mathbf{K}_{\mathbf{g}'}^{s'}$ . We note that the matrix elements  $S_{\mathbf{g}\mathbf{g}'}^{ss'}$  obey the symmetry relation  $S_{\mathbf{g}\mathbf{g}'}^{-s-s'} = S_{\mathbf{g}\mathbf{g}'}^{ss'}$ .

After calculating the transmitted and reflected waves, when a plane wave given by Eq. (9) is incident on the given plane of spheres, we can proceed to the calculation of the transmittance  $\mathcal{T}(\omega, \mathbf{k}_{\parallel} + \mathbf{g}')$  and the reflectance  $\mathcal{R}(\omega, \mathbf{k}_{\parallel} + \mathbf{g}')$  of the plane. These are defined as the ratio of the transmitted, respectively the reflected, energy flux to the energy flux associated with the incident wave. Assuming, e.g., incidence from the left we obtain

$$\mathcal{T} = \frac{\sum_{\mathbf{g}} |[U_{tr}]_{\mathbf{g}}^+|^2 K_{\mathbf{g}z}^+}{|[U_{in}]_{\mathbf{g}'}^+|^2 K_{\mathbf{g}'z}^+} \quad (19)$$

and

$$\mathcal{R} = \frac{\sum_{\mathbf{g}} |[U_{rf}]_{\mathbf{g}}^-|^2 K_{\mathbf{g}z}^+}{|[U_{in}]_{\mathbf{g}'}^+|^2 K_{\mathbf{g}'z}^+}. \quad (20)$$

We remember that only propagating beams (those with  $K_{\mathbf{g}z}^+$  real) enter the numerators of the above equations. Finally we note that if absorption is present it can be calculated from the requirement of energy conservation  $\mathcal{A} = 1 - (\mathcal{T} + \mathcal{R})$ .

The difference in the number of states up to a given frequency  $\omega$ , between the system under consideration (a plane of particles in a homogeneous medium) and that of the host medium extending over all space, is given by

$$\Delta N(\omega) = \frac{N}{A} \iint_{\text{SBZ}} d^2 k_{\parallel} \Delta N(\omega, k_{\parallel}), \quad (21)$$

where  $N$  is the number of surface unit cells of the plane particles and  $A$  the area of the SBZ. The  $\mathbf{k}_{\parallel}$ -resolved change in the number of states is given, in the spherical-wave representation, by [22]

$$\Delta N(\omega, \mathbf{k}_{\parallel}) = \frac{1}{\pi} \text{Im} \ln \det(\mathbf{I} + \mathbf{T}) - \frac{1}{\pi} \text{Im} \ln \det(\mathbf{I} - \mathbf{T}\mathbf{Z}), \quad (22)$$

where  $\mathbf{I}$  is the unit matrix, and in the plane wave representation by

$$\Delta N(\omega, \mathbf{k}_{\parallel}) = \frac{1}{2\pi} \text{Im} \ln \det \mathbf{S}. \quad (23)$$

We note that the  $S$  matrix is defined in the basis of those reciprocal-lattice vectors which correspond to propagating beams and that the resulting  $\Delta N(\omega, \mathbf{k}_{\parallel})$ , contrary to that

obtained through Eq. (22), does not include possible bound states of the system. The corresponding  $\mathbf{k}_{\parallel}$ -resolved change in the density of states is obtained through  $\Delta n(\omega, \mathbf{k}_{\parallel}) = \partial \Delta N(\omega, \mathbf{k}_{\parallel}) / \partial \omega$ .

In order to describe scattering by multilayers of particles with the same 2D periodicity, it is convenient to express the waves on the left of a given layer with respect to an origin,  $\mathbf{A}_l$ , on the left of the layer at  $-\mathbf{d}_l$  from its center and the waves on the right of this layer with respect to an origin,  $\mathbf{A}_r$ , on the right of the layer at  $\mathbf{d}_r$  from its center, i.e., a plane wave on the left of the layer will be written as  $\widehat{\mathbf{K}}_g^s U_g^s \exp[i\mathbf{K}_g^s \cdot (\mathbf{r} - \mathbf{A}_l)]$  and a plane wave on the right of the layer will be written as  $\widehat{\mathbf{K}}_g^s U_g^s \exp[i\mathbf{K}_g^s \cdot (\mathbf{r} - \mathbf{A}_r)]$ . With the above choice of origins the transmission (reflection) matrix elements of a layer become

$$\begin{aligned} Q_{gg'}^I &= S_{gg'}^{++} \exp[i(\mathbf{K}_g^+ \cdot \mathbf{d}_r + \mathbf{K}_g^+ \cdot \mathbf{d}_l)], \\ Q_{gg'}^{II} &= S_{gg'}^{+-} \exp[i(\mathbf{K}_g^+ \cdot \mathbf{d}_r - \mathbf{K}_g^- \cdot \mathbf{d}_r)], \\ Q_{gg'}^{III} &= S_{gg'}^{-+} \exp[-i(\mathbf{K}_g^- \cdot \mathbf{d}_l - \mathbf{K}_g^+ \cdot \mathbf{d}_l)], \\ Q_{gg'}^{IV} &= S_{gg'}^{--} \exp[-i(\mathbf{K}_g^- \cdot \mathbf{d}_l + \mathbf{K}_g^- \cdot \mathbf{d}_r)]. \end{aligned} \quad (24)$$

The transmission (reflection) matrices for a multilayer slab are obtained from the corresponding matrices of the individual layers, in the manner described in Ref. [18]. For a plane wave  $\widehat{\mathbf{K}}_g^+ [U_{in}]_g^+ \exp[i\mathbf{K}_g^+ \cdot (\mathbf{r} - \mathbf{A}_L)]$ , incident on the slab from the left, we finally obtain a reflected wave  $\sum_g \widehat{\mathbf{K}}_g^- [U_{rf}]_g^- \exp[i\mathbf{K}_g^- \cdot (\mathbf{r} - \mathbf{A}_L)]$  on the left of the slab and a transmitted wave  $\sum_g \widehat{\mathbf{K}}_g^+ [U_{tr}]_g^+ \exp[i\mathbf{K}_g^+ \cdot (\mathbf{r} - \mathbf{A}_R)]$  on the right of the slab, where  $\mathbf{A}_L$  ( $\mathbf{A}_R$ ) is the appropriate origin at the left (right) interface of the slab. We have

$$[U_{tr}]_g^+ = Q_{gg'}^I [U_{in}]_g^+ \quad (25)$$

and

$$[U_{rf}]_g^- = Q_{gg'}^{III} [U_{in}]_g^+, \quad (26)$$

where  $\mathbf{Q}^I$  and  $\mathbf{Q}^{III}$  are the appropriate transmission and reflection matrices of the slab. After calculating the transmitted and reflected waves on the right and left of the slab, we can obtain the corresponding transmittance  $T(\omega, \mathbf{k}_{\parallel} + \mathbf{g}')$  and the reflectance  $\mathcal{R}(\omega, \mathbf{k}_{\parallel} + \mathbf{g}')$  from Eqs. (19) and (20), respectively. On the other hand, the change in the number of states between the slab and the homogeneous host medium extending all over space can be calculated from Eqs. (21) and (23), where the elements of the  $S$  matrix in the plane-wave representation are given by

$$\begin{aligned} S_{gg'}^{++} &= \exp[-i(\mathbf{K}_g^+ \cdot \mathbf{A}_R - \mathbf{K}_g^+ \cdot \mathbf{A}_L)] Q_{gg'}^I, \\ S_{gg'}^{+-} &= \exp[-i(\mathbf{K}_g^+ \cdot \mathbf{A}_R - \mathbf{K}_g^- \cdot \mathbf{A}_R)] Q_{gg'}^{II}, \\ S_{gg'}^{-+} &= \exp[-i(\mathbf{K}_g^- \cdot \mathbf{A}_L - \mathbf{K}_g^+ \cdot \mathbf{A}_L)] Q_{gg'}^{III}, \\ S_{gg'}^{--} &= \exp[-i(\mathbf{K}_g^- \cdot \mathbf{A}_L - \mathbf{K}_g^- \cdot \mathbf{A}_R)] Q_{gg'}^{IV}, \end{aligned} \quad (27)$$

for the given  $\omega$  and  $\mathbf{k}_{\parallel}$ . The phase factors in Eq. (27) arise from the need to refer all waves to a common origin. The possible eigenmodes of the slab are obtained by requiring existence of a wave field localized within the slab in the absence of incident wave. Dividing the slab into a left and a right part, described by reflection matrices  $\mathbf{Q}_1^{II}$  and  $\mathbf{Q}_2^{III}$ , respectively, this requirement

leads to the secular equation

$$\det[\mathbf{I} - \mathbf{Q}_1^{II} \mathbf{Q}_2^{III}] = 0. \quad (28)$$

For a three-dimensional crystal consisting of an infinite periodic sequence of layers stacked along the  $z$  direction, the wave field in the host region between the  $n$ th and the  $(n+1)$ th unit slabs has the form  $\mathbf{U}(\mathbf{r}) = \sum_g \{\widehat{\mathbf{K}}_g^+ U_{gn}^+ \exp[i\mathbf{K}_g^+ \cdot (\mathbf{r} - \mathbf{A}_n)] + \widehat{\mathbf{K}}_g^- U_{gn}^- \exp[i\mathbf{K}_g^- \cdot (\mathbf{r} - \mathbf{A}_n)]\}$ , where  $\mathbf{A}_n$  is an appropriate origin between the  $n$ th and the  $(n+1)$ th unit slabs. The coefficients  $U_{gn}^{\pm}$  are obviously related to  $U_{g,n+1}^{\pm}$  through the  $\mathbf{Q}$  matrices of the unit slab as follows:

$$\begin{aligned} U_{g,n+1}^+ &= \sum_{g'} [Q_{gg'}^I U_{g'n}^+ + Q_{gg'}^{II} U_{g'n+1}^-], \\ U_{g'n}^- &= \sum_{g'} [Q_{gg'}^{III} U_{g'n}^+ + Q_{gg'}^{IV} U_{g'n+1}^-]. \end{aligned} \quad (29)$$

On the other hand, Bloch's theorem implies that  $U_{g,n+1}^{\pm} = \exp(i\mathbf{k} \cdot \mathbf{a}_3) U_{gn}^{\pm}$ , where  $\mathbf{a}_3$  is a vector which connects a point in the  $n$ th slab to an equivalent point in the  $(n+1)$ th slab and  $\mathbf{k} = (\mathbf{k}_{\parallel}, k_z(\omega, \mathbf{k}_{\parallel}))$ . For given  $\omega$  and  $\mathbf{k}_{\parallel}$  one can obtain  $k_z$  from the following eigenvalue equation:

$$\begin{aligned} &\begin{pmatrix} \mathbf{Q}^I & \mathbf{Q}^{II} \\ -[\mathbf{Q}^{IV}]^{-1} \mathbf{Q}^{III} \mathbf{Q}^I & [\mathbf{Q}^{IV}]^{-1} [\mathbf{I} - \mathbf{Q}^{III} \mathbf{Q}^{II}] \end{pmatrix} \begin{pmatrix} \mathbf{U}_n^+ \\ \mathbf{U}_{n+1}^- \end{pmatrix} \\ &= \exp(i\mathbf{k} \cdot \mathbf{a}_3) \begin{pmatrix} \mathbf{U}_n^+ \\ \mathbf{U}_{n+1}^- \end{pmatrix}, \end{aligned} \quad (30)$$

which follows directly from Eq. (29) and Bloch's theorem. Alternatively, one can formulate an eigenvalue equation for the transfer matrix,

$$\begin{aligned} &\begin{pmatrix} \mathbf{Q}^I - \mathbf{Q}^{II} [\mathbf{Q}^{IV}]^{-1} \mathbf{Q}^{III} & \mathbf{Q}^{II} [\mathbf{Q}^{IV}]^{-1} \\ -[\mathbf{Q}^{IV}]^{-1} \mathbf{Q}^{III} & [\mathbf{Q}^{IV}]^{-1} \end{pmatrix} \begin{pmatrix} \mathbf{U}_n^+ \\ \mathbf{U}_n^- \end{pmatrix} \\ &= \exp(i\mathbf{k} \cdot \mathbf{a}_3) \begin{pmatrix} \mathbf{U}_n^+ \\ \mathbf{U}_n^- \end{pmatrix}. \end{aligned} \quad (31)$$

The solutions  $k_z(\omega, \mathbf{k}_{\parallel})$  resulting from Eq. (30) or, equivalently, Eq. (31), looked upon as functions of real  $\omega$ , define for each  $\mathbf{k}_{\parallel}$  lines in the complex  $k_z$  plane, which all together constitute the complex band structure of the infinite crystal associated with the given crystallographic plane. A line of given  $\mathbf{k}_{\parallel}$  may be real (in the sense that  $k_z$  is real) over certain frequency regions, and be complex (in the sense that  $k_z$  is complex) for  $\omega$  outside these regions. It turns out that, for given  $\mathbf{k}_{\parallel}$  and  $\omega$ , out of the solutions  $k_z(\omega, \mathbf{k}_{\parallel})$ , none or, at best, a few are real and the corresponding eigenvectors represent propagating modes of the acoustic field in the given infinite crystal. The remaining solutions  $k_z(\omega, \mathbf{k}_{\parallel})$  are complex and the corresponding eigenvectors represent evanescent waves. These have an amplitude which increases exponentially in the positive or negative  $z$  direction and, unlike the propagating waves, do not exist as physical entities in the infinite crystal. However, they are an essential part of the physical solutions of the acoustic field in the case of a surface or a slab of finite thickness. A region of frequency where propagating waves do not exist, for given  $\mathbf{k}_{\parallel}$ , constitutes a frequency gap of the acoustic field for the given  $\mathbf{k}_{\parallel}$ . If over a frequency region no propagating wave exists whatever the



value of  $\mathbf{k}_{\parallel}$ , then this region constitutes an absolute frequency gap.

Finally, for the sake of completeness, we note that the transfer matrix on the left hand side of Eq. (31) can also provide the reflection matrix,  $\mathbf{R}_{\infty}$ , of the corresponding semi-infinite crystal and, through  $\mathbf{R}_{\infty}$ , one can find the surface states of the crystal, if such exist. In order to obtain  $\mathbf{R}_{\infty}$ , the eigenvectors of the transfer matrix need to be arranged in a matrix  $\mathbf{F}$  which projects the space of forward and backward Bloch eigenmodes,  $\mathbf{V}^+$  and  $\mathbf{V}^-$ , onto the original plane-wave basis, as follows [27,28]:

$$\begin{pmatrix} \mathbf{U}_0^+ \\ \mathbf{U}_0^- \end{pmatrix} = \begin{pmatrix} \mathbf{F}^{++} & \mathbf{F}^{+-} \\ \mathbf{F}^{-+} & \mathbf{F}^{--} \end{pmatrix} \begin{pmatrix} \mathbf{V}^+ \\ \mathbf{V}^- \end{pmatrix}. \quad (32)$$

By definition, each eigenmode propagates through the crystal without changing its state and, on the other hand, for a semi-infinite crystal, there is no rear surface to reflect the forward into backward Bloch waves. Therefore, the appropriate boundary condition for the scattering problem of an acoustic wave incident on a semi-infinite phononic crystal from the homogeneous host material that extends to infinity is  $\mathbf{V}^- = 0$  [28]. Therefore, Eq. (32) yields

$$\mathbf{U}_0^- = \mathbf{F}^{-+}[\mathbf{F}^{++}]^{-1}\mathbf{U}_0^+ \equiv \mathbf{R}_{\infty}\mathbf{U}_0^+. \quad (33)$$

On the other hand, the condition for the occurrence of surface states translates to the existence of nonzero forward Bloch modes ( $\mathbf{V}^+ \neq 0$ ) in the absence of incoming field ( $\mathbf{U}_0^+ = 0$ ) [29,30]. Then Eq. (32) gives  $\mathbf{F}^{++}\mathbf{V}^+ = \mathbf{U}_0^+ = 0$ , which is satisfied when  $\det[\mathbf{F}^{++}] = 0$ .

### III. RESULTS AND DISCUSSION

In this work we report a thorough theoretical study of the acoustic properties of a specific water-saturated double-porosity granular polymeric structure consisting of close-packed porous polystyrene spheres, with porosity  $f$  and diameter  $D$ , in the [111] fcc stacking. In this geometry  $D = a\sqrt{2}/2$ , where  $a$  is the fcc lattice constant, while consecutive (111) fcc planes are separated by a distance  $d = D\sqrt{6}/3$ . The values of the relevant parameters of the solid (denoted by an index  $s$ ) and fluid (denoted by an index  $f$ ), which coincides with the host (denoted by an index  $h$ ), materials involved are as follows: mass density  $\rho_s = 1050 \text{ kg m}^{-3}$ , longitudinal wave velocity  $c_{sl} = \sqrt{(K_s + 4\mu_s/3)/\rho_s} = 2350 \text{ ms}^{-1}$ , transverse wave velocity  $c_{st} = \sqrt{\mu_s/\rho_s} = 1200 \text{ ms}^{-1}$ , for polystyrene; and mass density  $\rho_f = 1000 \text{ kg m}^{-3}$  (longitudinal) wave velocity  $c_f = \sqrt{K_f/\rho_f} = 1480 \text{ ms}^{-1}$ , and fluid viscosity  $\eta = 10^{-3} \text{ Pa s}$ , for water. The elastic moduli of the bare skeletal frame of the porous polystyrene spheres,  $K_b$  and  $\mu_b$ , can be experimentally measured independently. However, since there are no experimental data available, following Kargl and Lim [16], we evaluate them using Berryman's self-consistent effective medium theory for a polystyrene/void elastic composite, assuming that the pores are modeled by randomly distributed needles, as appropriate for the low-porosity limit that will concern us here [31,32]. For example, for  $f = 10\%$  that we will consider in our study, we find  $K_b = 2.602 \text{ GPa}$  and  $\mu_b = 1.186 \text{ GPa}$ . Accordingly, the tortuosity is given by  $\alpha = f^{-2/3}$ , for a random array of needles [33]. Our

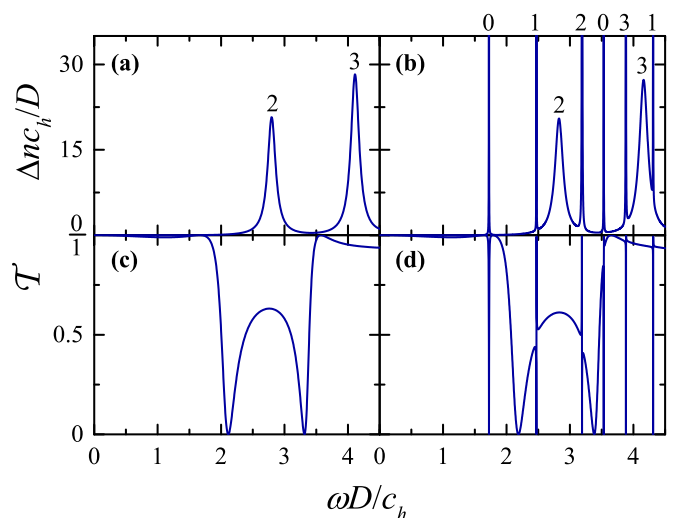


FIG. 1. (Upper diagrams) Change in the density of states of the acoustic field [Eq. (6)] induced by a submerged water-saturated porous polystyrene sphere, with porosity  $f = 10\%$ , (a) treated as a lossless homogeneous sphere with elastic parameters evaluated using self-consistent effective-medium theory for composite elastic media [31,32] and (b) described by Biot's theory, ignoring viscous losses ( $\eta = 0$ ). The peaks in (a) and (b) correspond to resonances of given multipole order,  $\ell$ , denoted in the diagrams. (Lower diagrams) Transmittance of an acoustic plane wave [Eq. (19)] incident normally on a hexagonal array, i.e., a single fcc (111) plane, of the above spheres. In (c) and (d) the spheres are described as in (a) and (b), respectively.

numerical calculations are carried out by the layer-multiple-scattering method described in Sec. II, where we truncated the spherical-wave expansions at  $\ell_{\max} = 7$  and took into account 43 2D reciprocal lattice vectors in the relevant plane-wave expansions, thus ensuring good convergence in all cases examined.

In Biot's theory [9,10], by which we describe the individual porous spheres, there are two distinct limits. When the viscous skin depth,  $\delta = \sqrt{2\eta/(\omega\rho_f)}$ , is much larger than the radius,  $R_p$ , of the (cylindrical) pores, viscous drag prevents the efficient formation of slow longitudinal waves, which are associated with an out-of-phase relative motion of the solid frame and infiltrated liquid. In this so-called viscous-coupling limit, the porous material behaves as an effective homogeneous medium, the elastic parameters of which can be evaluated, e.g., by the self-consistent homogenization method of Berryman [31,32], while dissipative losses are quite small and can be neglected [16]. On the other hand, when  $\delta \ll R_p$ , we are in the so-called inertial-coupling limit where all three bulk acoustic modes in the porous material (transverse, fast, and slow longitudinal) become nondispersive and attenuation free, as one would have in the absence of viscous losses ( $\eta = 0$ ).

The change in the density of states of the acoustic field induced by a submerged water-saturated porous polystyrene sphere and the acoustic transmission spectrum of a 2D hexagonal array of such close-packed spheres, at normal incidence, in the above two limits are depicted in Fig. 1. Since in these lossless cases there is no characteristic length scale in the problem, the results apply to different regions of

frequency provided that the dimensions of the structural units are scaled accordingly. Therefore, we choose to represent our results using  $\omega D/c_h$  as dimensionless frequency.

The eigenmodes of the acoustic field in the case of a single sphere, i.e., solutions of Eq. (4) in the absence of an incident field, are obtained at the poles of the scattering  $T$  matrix. Besides the torsional bound states with real eigenfrequencies, which are confined in the sphere and cannot be excited by an externally incident wave [34], there are resonant modes at the poles of the  $T$  matrix in the lower complex frequency half-plane, near the real axis, at  $z_\ell = \omega_\ell - i\gamma_\ell$ ;  $\omega_\ell$  is the eigenfrequency while  $\gamma_\ell$  denotes the inverse of the lifetime of the respective  $2^\ell$ -pole resonant mode. The corresponding change in the density of states can be deduced from Eq. (5) through a Laurent expansion in the vicinity of  $z_\ell$  on the real axis, which yields  $\Delta n_\ell(\omega) \simeq \frac{(2\ell+1)}{\pi} \gamma_\ell / [(\omega - \omega_\ell)^2 + \gamma_\ell^2]$ , i.e., the change of the partial density of states,  $\Delta n_\ell(\omega)$ , is a Lorentzian centered at  $\omega_\ell$  with a half width at half maximum equal to  $\gamma_\ell$ . These resonant modes, when the spheres are assembled in a 2D lattice, form bands  $\omega_\nu(\mathbf{k}_\parallel)$ ,  $\nu = 1, 2, \dots$  of corresponding collective modes of the plane. In our case, at  $\mathbf{k}_\parallel = 0$ , the hexagonal symmetry of the structure implies that there will be a partial lift of the  $(2\ell + 1)$  fold degeneracy of the resonant modes of the individual spheres and the corresponding modes of the plane will have the symmetry of the irreducible representations of the  $C_{6v}$  point group:  $L_1, L_1', L_2, L_2'$  (one dimensional) and  $L_3, L_3'$  (two dimensional) [35]. Therefore, they will be either nondegenerate or doubly degenerate, respectively. We note that only the  $L_1$  modes are acoustically active in the sense that they can be excited by an acoustic plane wave with appropriate frequency incident normally on the given plane, because they have the proper symmetry [36] and manifest themselves as resonance structures in the corresponding transmission spectrum. The acoustically inactive, so-called deaf, modes are bound states with infinite lifetime, confined in the plane, and cannot be excited by an externally incident wave. However, for  $\mathbf{k}_\parallel \neq 0$ , a general non-high-symmetry point, all modes belong to the identity representation of the trivial group and, therefore, are acoustically active.

As shown in Figs. 1(a) and 1(c), in the viscous-coupling limit, we obtain the typical acoustic response of nonporous polymer spheres characterized by well-formed resonances, which originate from the spheroidal modes of the individual particles [36,37] and move to lower frequencies with increasing porosity. On the contrary, in the inertial-coupling limit, interestingly, additional very sharp resonances appear in the transmission spectrum of a hexagonal array, i.e., a single fcc (111) plane, of submerged water-saturated close-packed porous polystyrene spheres, with porosity  $f = 10\%$ , as can be seen in Fig. 1(d). These resonances stem from corresponding single-particle modes [see Fig. 1(b)] with a very long lifetime, which are strongly localized in the spheres and have a predominant character of slow longitudinal waves. Therefore, these modes, which are pushed up to higher frequencies with increasing porosity, should be unambiguously ascribed to the existence of slow longitudinal waves in the poroelastic particles. As expected from a group-theory analysis [35], each sphere mode of  $\ell = 0, 1, 2, 3$  gives one acoustically active  $L_1$  mode of the given planar array for  $\mathbf{k}_\parallel = 0$ , as can be seen

TABLE I. Compatibility relations between irreducible representations of the  $O(3)$ ,  $C_{6v}$ , and  $C_{3v}$  point symmetry groups.

$O(3)$	$\ell = 0$	$\ell = 1$	$\ell = 2$	$\ell = 3$
$C_{6v}$	$L_1$	$L_1 L_{3'}$	$L_1 L_3 L_{3'}$	$L_1 L_2 L_2' L_3 L_{3'}$
$C_{3v}$	$\Lambda_1$	$\Lambda_1 \Lambda_{3'}$	$\Lambda_1 \Lambda_3 \Lambda_{3'}$	$\Lambda_1 \Lambda_2 \Lambda_2' \Lambda_3 \Lambda_{3'}$

in Fig. 1. In addition, there are acoustically inactive plane modes of different symmetry, as implied from the appropriate compatibility relations (see Table I).

In the case of a pair of two consecutive fcc (111) planes of the spheres under consideration, for given  $\mathbf{k}_\parallel$ , each plane mode gives rise to two modes due to interlayer coupling, by analogy to the formation of bonding and antibonding orbitals of a diatomic molecule from the corresponding electronic states of the individual atoms, as depicted in Fig. 2 for  $\mathbf{k}_\parallel = 0$ . By the same token, by stacking consecutive hexagonal arrays so as to grow an infinite fcc crystal of submerged water-saturated close-packed porous polystyrene spheres, the modes of the individual planes will form corresponding bands.

For  $\mathbf{k}_\parallel = 0$  the bands have the symmetry of the irreducible representations of the  $C_{3v}$  point group [35]. Therefore, they are either nondegenerate, if they have the  $\Lambda_1$  or the  $\Lambda_2$  symmetry, or doubly degenerate if they have the  $\Lambda_3$  symmetry. We note that only the  $\Lambda_1$  bands are acoustically active in the sense that they can be excited by an acoustic plane wave with appropriate frequency incident normally on a (111) slab of the crystal, which is then transmitted through

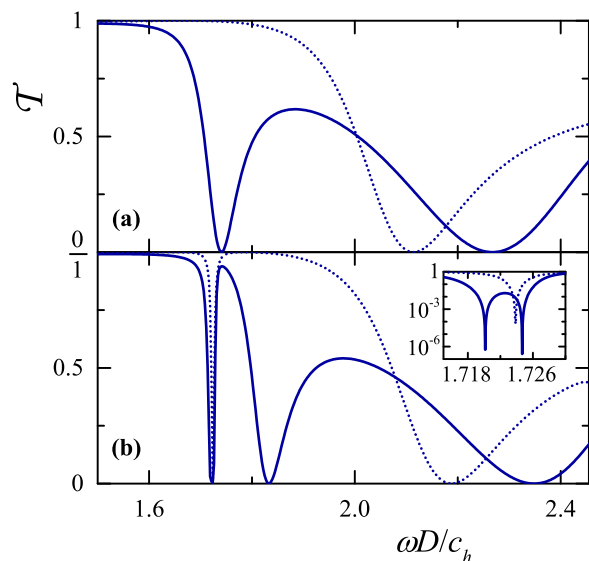


FIG. 2. Transmittance of an acoustic plane wave incident normally on a bilayer of consecutive fcc (111) planes of submerged water-saturated close-packed porous polystyrene spheres, with porosity  $f = 10\%$ , (a) treated as lossless homogeneous spheres with elastic parameters calculated using self-consistent effective-medium theory for composite elastic media [31,32] and (b) described by Biot's theory, ignoring viscous losses ( $\eta = 0$ ). The dotted lines in (a) and (b) display the corresponding transmission spectra for a single fcc (111) plane of such spheres. The inset to (b) shows an enlarged view about the sharp resonances in the low frequency part of the spectrum, in logarithmic scale.

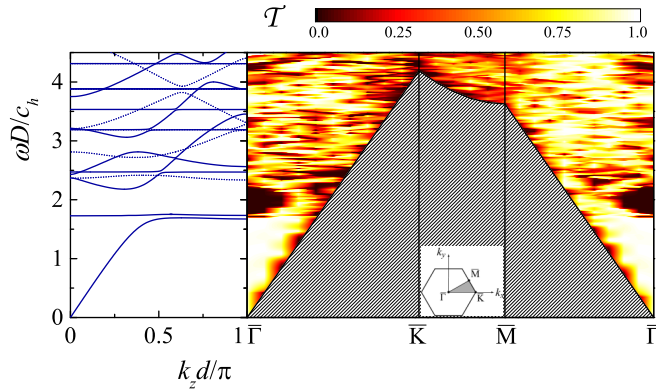


FIG. 3. (Left-hand diagram) Phononic dispersion diagram of an fcc crystal of submerged water-saturated close-packed porous polystyrene spheres, with porosity  $f = 10\%$ , described by Biot's theory without viscous losses ( $\eta = 0$ ), along the [111] direction. (Right-hand diagram) Transmittance of an acoustic plane wave incident on a (111) slab of this crystal, eight layers thick, with  $\mathbf{k}_{\parallel}$  along the high-symmetry lines of the corresponding SBZ, shown in the inset.  $\bar{\Gamma}$ :  $\mathbf{k}_{\parallel} = \frac{2\pi}{D}(0,0)$ ;  $\bar{K}$ :  $\mathbf{k}_{\parallel} = \frac{2\pi}{D}(\frac{2}{3},0)$ ;  $\bar{M}$ :  $\mathbf{k}_{\parallel} = \frac{2\pi}{D}(\frac{1}{2}, \frac{\sqrt{3}}{6})$ . The direction of incidence is specified by the corresponding polar angle,  $\theta = \arccos(\sqrt{1 - c_h^2 k_{\parallel}^2 / \omega^2})$ , and azimuthal angle,  $\phi = \arctan(k_y / k_x)$ , respectively. Obviously, at given  $\mathbf{k}_{\parallel}$ , propagating incident waves exist above an angular frequency threshold  $\omega_{inf} = c_h |\mathbf{k}_{\parallel}|$  (hatched area).

the slab, because they have the proper symmetry [36]. In addition to the above relatively narrow bands, there is an extended acoustic band, of  $\Lambda_1$  symmetry, which would be in a corresponding effective homogeneous medium, folded within the first Brillouin zone because of structure periodicity, with Bragg gaps appearing at the zone boundaries. Besides the Bragg gaps, when the extended acoustic band crosses a narrow band of the same symmetry, level repulsion leads, also, to the opening of a frequency gap about the crossing point, the so-called hybridization gap. Such a relatively wide hybridization gap appears, e.g., in the dispersion diagram, obtained by solving the eigenvalue problem (30), displayed in Fig. 3 about  $\omega D/c_h = 2$  for  $\mathbf{k}_{\parallel} = 0$ . However, as can be seen in Fig. 3, this gap is not omnidirectional. It progressively shrinks as we deviate from  $\mathbf{k}_{\parallel} = 0$  and finally closes, thus allowing for acoustic transmission through a finite slab of the crystal.

It is worth noting that specific features of the phononic band structure depicted in Fig. 3, such as anisotropy, flat bands, and frequency gaps driven by coherent multiple scattering, cannot be accounted for by any local effective-medium theory for double-porosity media. These theories are valid when the wavelength is much longer than the size of the representative elementary volume and describe the composite medium in terms of effective quantities. For example, the model of Berryman and Wang [38,39], in the absence of viscous losses ( $\eta = 0$ ) as appropriate for the case under consideration in Fig. 3, predicts the existence of one transverse and three longitudinal acoustic waves with frequency-independent propagation velocities. This model assumes a fluid-saturated double-porosity medium consisting of a porous matrix with fractures, where each of the three components, i.e., solid skeletal frame, matrix pores, and adjacent fractures, forms a percolating network. Therefore, there are indeed one transverse wave propagating

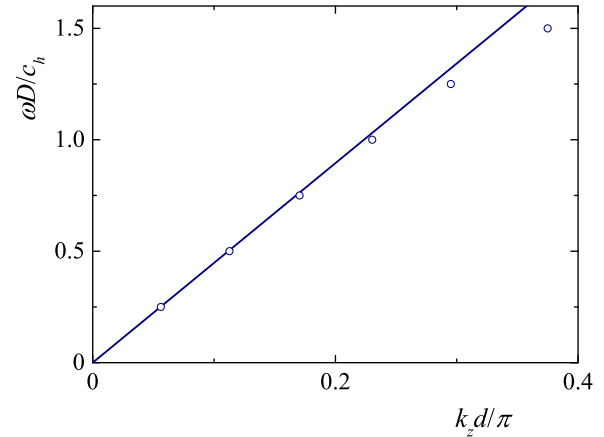


FIG. 4. Enlarged view of the left-hand diagram of Fig. 3 in the long-wavelength limit (symbols). The solid line shows the linear dispersion curve with slope  $\bar{c}$  calculated by Eq. (A10).

in the solid frame and three hybrid longitudinal waves, which arise from the corresponding propagating modes in the above three components interacting between them. In our case of unconsolidated porous polymer grains, the continuous network topology of the solid frame and the matrix pores is broken, and thus only the longitudinal acoustic wave propagating in the fluid-filled fractures will survive. The propagation velocity,  $\bar{c}$ , of this wave in the particular morphology of the granular double-porosity medium that concerns us here (and corresponds to vanishing elastic moduli of the solid skeletal frame [17]) can be deduced from the model of Berryman and Wang [38,39] (see the Appendix). As shown in Fig. 4,  $\bar{c}$ , evaluated by Eq. (A10), is in excellent agreement with the slope of the dispersion curve obtained by our layer-multiple-scattering calculations in the long-wavelength limit.

Viscous losses are described by Biot's theory [9,10], which properly combines both mechanical and hydrodynamic properties of a composite comprising a porous elastic medium filled with a viscous fluid. Strong absorption is expected in frequency regions where resonant modes localized in the spheres exist, especially if these modes have strong admixture of slow longitudinal waves, which correspond to an out-of-phase relative motion of the solid frame and infiltrated liquid in the porous material. As a typical example, in Fig. 5 we display the evolution of the absorption spectrum of a bilayer of consecutive fcc (111) planes of submerged water-saturated close-packed porous polystyrene spheres of diameter  $D = 5$  mm, with porosity  $f = 10\%$ , for different pore sizes, in the frequency region of the first resonant modes. For narrow pores ( $R_p = 500$  nm), we are in the viscous-coupling regime where slow longitudinal waves are not efficiently excited and thus a very weak absorption band is observed at the resonance which originates from the quadrupole spheroidal-like particle modes [see Fig. 5(a)]. As the pore radius increases, the slow-wave component of these modes is clearly manifested in a stronger absorption peak, which becomes prominent at  $R_p = 5$   $\mu$ m [see Fig. 5(b)]. By further increasing the pore radius well beyond the viscous length, which is about 2  $\mu$ m in the frequency region under consideration, the losses associated with the spheroidal-like particle modes are gradually suppressed. At the same time, the sharp particle modes, which have an almost exclusively

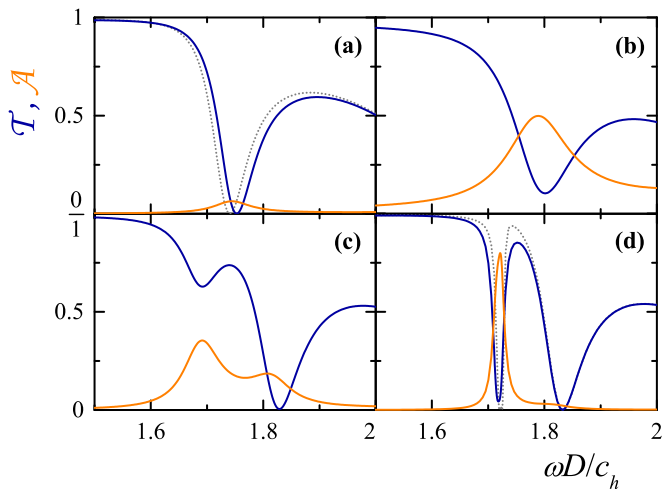


FIG. 5. Transmittance and absorbance of an acoustic plane wave incident normally on bilayer of consecutive fcc (111) planes of submerged water-saturated close-packed porous polystyrene spheres of diameter  $D = 5$  mm, with porosity  $f = 10\%$ , for different pore sizes:  $R_p = 500$  nm (a),  $R_p = 5$   $\mu\text{m}$  (b),  $R_p = 50$   $\mu\text{m}$  (c), and  $R_p = 500$   $\mu\text{m}$  (d). The dotted lines in (a) and (d) display the corresponding transmission spectra for homogeneous spheres with elastic parameters calculated using self-consistent effective-medium theory for (lossless) composite elastic media [31,32] and for water-saturated porous spheres described by Biot's theory, neglecting viscous losses ( $\eta = 0$ ), respectively.

slow-wave character in the spheres, are developed and manifest themselves as strong peaks in the absorption spectrum, as shown in Figs. 5(c) and 5(d) for the lowest monopole mode of this type in the range of frequencies considered. For wide pores, in the inertial-coupling regime, we obtain very narrow and dispersionless bands of strong absorption at the frequencies of these modes in the double-porosity polymeric material under consideration, as shown in Fig. 6.

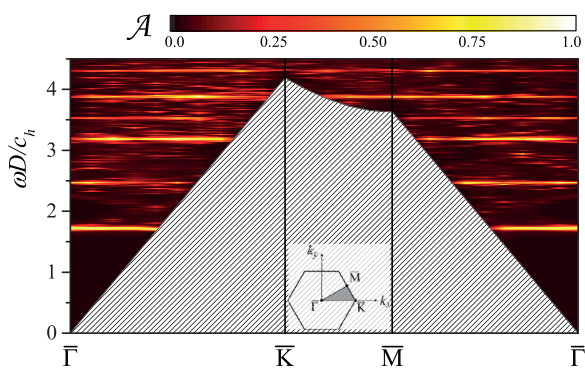


FIG. 6. Absorbance of an acoustic plane wave incident on a slab consisting of eight fcc (111) planes of submerged water-saturated close-packed porous polystyrene spheres ( $D = 5$  mm,  $f = 10\%$ , and  $R_p = 500$   $\mu\text{m}$ ) with  $\mathbf{k}_{\parallel}$  along the high-symmetry lines of the corresponding SBZ, shown in the inset.  $\bar{\Gamma}$ :  $\mathbf{k}_{\parallel} = \frac{2\pi}{D}(0,0)$ ;  $\bar{K}$ :  $\mathbf{k}_{\parallel} = \frac{2\pi}{D}(\frac{2}{3},0)$ ;  $\bar{M}$ :  $\mathbf{k}_{\parallel} = \frac{2\pi}{D}(\frac{1}{2},\frac{\sqrt{3}}{6})$ . The direction of incidence is specified by the corresponding polar angle,  $\theta = \arccos(\sqrt{1 - c_h^2 k_{\parallel}^2 / \omega^2})$ , and azimuthal angle,  $\phi = \arctan(k_y / k_x)$ , respectively. Obviously, at given  $\mathbf{k}_{\parallel}$ , propagating incident waves exist above an angular frequency threshold  $\omega_{inf} = c_h |\mathbf{k}_{\parallel}|$  (hatched area).

#### IV. CONCLUSIONS

In summary, we reported a thorough theoretical study of the acoustic response of a particular class of double-porosity liquid-saturated granular polymeric material, formed by close-packed porous polymer spheres assembled in an fcc lattice, by means of numerical calculations using a proper generalization of the layer-multiple-scattering method to structures of poroelastic spherical bodies, which are described by Biot's theory [9,10]. Calculated transmission and absorption spectra of finite slabs of these materials are analyzed by reference to the acoustic modes of the constituent spheres as well as to the dispersion diagrams of corresponding infinite crystals, providing a consistent interpretation of the observed features. In particular, our results reveal the existence of resonant modes with very long lifetime, localized in the spheres, in the inertial-coupling regime, i.e., when the radius of the spheres' pores is much larger than the viscous length. These modes, which can be easily tuned in frequency by adjusting the intrinsic porosity of the spheres, induce narrow dispersionless absorption bands as well as directional gaps in the transmission spectrum of finite slabs of the double-porosity material.

#### ACKNOWLEDGMENTS

A.A. was supported by the project SUPERMEN through a postgraduate fellowship. This project is co-financed by the European Union through the European Regional Development Fund and by the Conseil Regional de Haute Normandie.

#### APPENDIX

The double-porosity water-saturated polymer structure under study can be viewed as a special case of the model presented in Refs. [38,39], whose terminology and notation we adopt here to facilitate comparison. Our unconsolidated fluid-saturated polymer spheres correspond to the porous matrix (called "phase 1" in Ref. [38]) and the interstitial void space filled by water corresponds to the water-filled fractures (called "phase 2" in Ref. [38]), occupying, respectively, fractional volumes  $v^{(1)} \equiv v$  and  $v^{(2)} \equiv 1 - v$ . We shall derive the expression for the effective-medium velocity for such a crystal, in the case where viscous losses are neglected. The condition of perfect locking in the motion between the solid and the two fluid components, valid in the long-wavelength regime that interests us here, implies  $\mathbf{u} = \mathbf{U}^{(s)}$  for the corresponding displacement fields of the solid and two fluids ( $s = 1$  for the fluid in the matrix pores and  $s = 2$  for the fluid in the fractures). Thus the total kinetic energy of the system is written as  $T = \frac{1}{2} \rho_{tot} \dot{\mathbf{u}} \cdot \dot{\mathbf{u}}$ , where  $\rho_{tot} = v(1 - f)\rho_s + [1 - v(1 - f)]\rho_f$  is the total inertia of the system, and use of Lagrange's equation leads to the following expression for the stress tensor (a  $e^{-i\omega t}$  dependence is assumed):

$$\tau_{i,j} = \partial_t \partial_{\hat{u}_i} T = -\omega^2 \rho_{tot} u_i. \quad (\text{A1})$$

On the other hand, the weak-frame approximation ( $K, \mu \rightarrow 0$ ), valid for unconsolidated grains, yields [see Eqs. (29) and (30) of Ref. [39]]

$$\tau_{i,j} = -p_{c,i}, \quad (\text{A2})$$



with  $p_c$  being the confining pressure applied to the boundaries of the whole structure. Combining Eqs. (A1) and (A2) and since, by definition, the dilatational strain  $e = u_{i,i}$ , and,  $p_{c,ii} = -k^2 p_c$ , with  $k$  being the wave number, we obtain the effective-medium velocity

$$\bar{c}^2 = \lim_{\omega \rightarrow 0} \left( \frac{\omega}{k} \right)^2 = -\frac{p_c}{e} \frac{1}{\rho_{\text{tot}}}. \quad (\text{A3})$$

The initial condition  $\mathbf{u} = \mathbf{U}^{(s)}$ , or, equivalently,  $\zeta^{(s)} = 0$ ,  $s = 1, 2$ , for the two fluid contents, arising from the long-wavelength regime, leads to a simplified form for the stress-strain phenomenological linear system, described by Eq. (27) of Ref. [39], which, in the general case of the unconsolidated-grain limit, is written as

$$\begin{pmatrix} -p_c \\ -p_f^{(1)} \\ -p_f^{(2)} \end{pmatrix} = \begin{pmatrix} \tilde{a}_{11} & \tilde{a}_{12} & \tilde{a}_{11} \\ \tilde{a}_{12} & \tilde{a}_{22} & \tilde{a}_{12} \\ \tilde{a}_{11} & \tilde{a}_{12} & \tilde{a}_{11} \end{pmatrix} \begin{pmatrix} e \\ -\zeta^{(1)} \\ -\zeta^{(2)} \end{pmatrix}. \quad (\text{A4})$$

In the above expression,  $\tilde{a}_{ij}$  are the inverse-matrix elements of the matrix defined in Eq. (27) of Ref. [39], and  $p_f^{(s)}$  are the pressures in the fluids of each phase  $s$ . Indeed, Eq. (A4) reduces to the form

$$\begin{pmatrix} -p_c \\ -p_f^{(1)} \\ -p_f^{(2)} \end{pmatrix} = \begin{pmatrix} \tilde{a}_{11} \\ \tilde{a}_{12} \\ \tilde{a}_{11} \end{pmatrix} e, \quad (\text{A5})$$

from which  $p_c = p_f^{(2)} = -\tilde{a}_{11}e$  (being naturally expected, since, in the unconsolidated-grain limit, phase 2 completely surrounds phase 1) and  $p_f^{(1)} = p_c \frac{\tilde{a}_{12}}{\tilde{a}_{11}}$ . Explicit expressions for  $\tilde{a}_{11}$ ,  $\tilde{a}_{12}$  can be found to be [see Eqs. (60)–(69) of Ref. [38]]

$$\tilde{a}_{11} \equiv \mathcal{D}^{-1}(a_{22}a_{33} - a_{23}^2) = \frac{\tilde{a}_{12}}{B^{(1)}}, \quad (\text{A6})$$

$$\tilde{a}_{12} \equiv \mathcal{D}^{-1}(a_{13}a_{23} - a_{12}a_{33}) = B^{(1)} \left[ \frac{1-v}{K_f} + \frac{v}{K_u^{(1)}} \right]^{-1}, \quad (\text{A7})$$

where  $\mathcal{D} = a_{11}a_{22}a_{33} + 2a_{12}a_{13}a_{23} - a_{11}a_{23}^2 - a_{22}a_{13}^2 - a_{33}a_{12}^2$ ,

$$\frac{1}{K_u^{(1)}} = \frac{1 - \alpha^{(1)} B^{(1)}}{K^{(1)}}, \quad (\text{A8})$$

the inverse *undrained* modulus for phase 1 and,  $\alpha^{(1)}$  and  $B^{(1)}$ , the corresponding Biot-Willis and Skempton coefficients, respectively. Combining the above expressions (A5)–(A8) we find  $p_f^{(1)} = p_c B^{(1)}$  and

$$-\frac{p_c}{e} = \tilde{a}_{11} = \left[ \frac{1-v}{K_f} + \frac{v}{K_u^{(1)}} \right]^{-1}. \quad (\text{A9})$$

After substitution of Eq. (A9) in (A3) we finally obtain the effective-medium velocity at the long wavelength regime for the double-porosity medium in the unconsolidated-grain limit as

$$\bar{c}^2 = \lim_{\omega \rightarrow 0} \left( \frac{\omega}{k} \right)^2 = \frac{K_{\text{eff}}}{\rho_{\text{eff}}}, \quad (\text{A10})$$

where the effective elastic parameters are defined by

$$\frac{1}{K_{\text{eff}}} \equiv \frac{1-v}{K_f} + \frac{v}{K_u^{(1)}}, \quad (\text{A11})$$

$$\rho_{\text{eff}} \equiv \rho_{\text{tot}}. \quad (\text{A12})$$

The quantity  $K_{\text{eff}}^{-1}$  has a clear physical meaning, being an average-law contribution of the two phases: that of the host fluid (fractures) and that of the porous water-saturated undrained spheres (porous matrix). In the case of close-packed ( $v = 0.74$ ) polystyrene spheres immersed in water we obtain  $\rho_{\text{eff}} = 1.0333\rho_f$ ,  $K_{\text{eff}} = 1.397K_f$ , and  $\bar{c} = 1721 \text{ ms}^{-1}$ , the latter being in excellent agreement with the value deduced from our multiple-scattering calculations,  $\bar{c} = 1717 \text{ ms}^{-1}$ .

- 
- [1] *Hierarchically Structured Porous Materials*, edited by B. L. Su, C. Sanchez, and X. Y. Yang (Wiley-VCH Verlag GmbH & Co. KGaA, Weinheim, 2011).
- [2] H. Sai, K. W. Tan, K. Hur, E. Asenath-Smith, R. Hovden, Y. Jiang, M. Riccio, D. A. Muller, V. Esler, L. A. Estroff, S. M. Gruner, and U. Wiesner, *Science* **341**, 530 (2013).
- [3] M. Sušec, S. C. Ligon, J. Stampfl, R. Liska, and P. Krajnc, *Macromol. Rapid Commun.* **34**, 938 (2013).
- [4] J. Wang, B. H. Lessard, M. Maric, and B. D. Favis, *Polymer* **55**, 3461 (2014).
- [5] J. F. Gao, J. S. P. Wong, M. J. Hu, W. Li, and R. K. Y. Li, *Nanoscale* **6**, 1056 (2014).
- [6] M. G. Seo, S. B. Kim, J. H. Oh, S. J. Kim, and M. A. Hillmyer, *J. Am. Chem. Soc.* **137**, 600 (2015).
- [7] S. A. Saba, M. P. S. Mousavi, P. Bühlmann, and M. A. Hillmyer, *J. Am. Chem. Soc.* **137**, 8896 (2015).
- [8] C. Y. Park, Y. J. La, T. H. An, Y. Jeong, S. Y. Kang, S. H. Joo, H. J. Ahn, T. J. Shin, and K. T. Kim, *Nat. Commun.* **6**, 6392 (2015).
- [9] M. A. Biot, *J. Acoust. Soc. Am.* **28**, 168 (1956).
- [10] M. A. Biot, *J. Acoust. Soc. Am.* **28**, 179 (1956).
- [11] C. Boutin and P. Royer, *Geophys. J. Int.* **203**, 1694 (2015).
- [12] H. Franklin, F. Luppé, and J. M. Conoir, *J. Acoust. Soc. Am.* **135**, 2513 (2014).
- [13] V. H. Nguyen, E. Rohan, and S. Naili, *Int. J. Eng. Sci.* **101**, 92 (2016).
- [14] R. Venegas and O. Umnova, *J. Acoust. Soc. Am.* **130**, 2765 (2011).
- [15] F. Chevillotte, C. Perrot, and E. Guillon, *J. Acoust. Soc. Am.* **134**, 4681 (2013).
- [16] S. G. Kargl and R. Lim, *J. Acoust. Soc. Am.* **94**, 1527 (1993).

- [17] D. L. Johnson and T. J. Plona, *J. Acoust. Soc. Am.* **72**, 556 (1982).
- [18] I. E. Psarobas, N. Stefanou, and A. Modinos, *Phys. Rev. B* **62**, 278 (2000).
- [19] R. Sainidou, N. Stefanou, I. E. Psarobas, and A. Modinos, *Comput. Phys. Commun.* **166**, 197 (2005).
- [20] A. Alevizaki, R. Sainidou, P. Rembert, B. Morvan, and N. Stefanou, *Phys. Rev. B* **94**, 174306 (2016).
- [21] M. Abramowitz and I. A. Stegun, *Handbook of Mathematical Functions* (Dover, New York, 1965).
- [22] R. Sainidou, N. Stefanou, and A. Modinos, *Phys. Rev. B* **69**, 064301 (2004).
- [23] I. E. Psarobas, *Phys. Rev. B* **64**, 012303 (2001).
- [24] J. B. Pendry, *Low Energy Electron Diffraction* (Academic Press, London, 1974).
- [25] C. M. Linton and I. Thompson, *J. Comput. Phys.* **228**, 1815 (2009).
- [26] B. Stout and R. McPhedran, *Wave Motion* **70**, 29 (2017).
- [27] C. Tserkezis and N. Stefanou, *Phys. Rev. B* **81**, 115112 (2010).
- [28] Z. Y. Li and K. M. Ho, *Phys. Rev. B* **68**, 155101 (2003).
- [29] C. Tserkezis, N. Stefanou, G. Gantzounis, and N. Papanikolaou, *Phys. Rev. B* **84**, 115455 (2011).
- [30] F. J. Lawrence, L. C. Botten, K. B. Dossou, R. C. McPhedran, and C. M. de Sterke, *Phys. Rev. A* **82**, 053840 (2010).
- [31] J. G. Berryman, *J. Acoust. Soc. Am.* **68**, 1809 (1980).
- [32] J. G. Berryman, *J. Acoust. Soc. Am.* **68**, 1820 (1980).
- [33] P. N. Sen, C. Scala, and M. H. Cohen, *Geophysics* **46**, 781 (1981).
- [34] H. Lamb, *Proc. London Math. Soc.* **s1-13**, 189 (1882).
- [35] J. F. Cornwell, *Group Theory and Electronic Energy Bands in Solids* (North-Holland, Amsterdam, 1969).
- [36] I. E. Psarobas, A. Modinos, R. Sainidou, and N. Stefanou, *Phys. Rev. B* **65**, 064307 (2002).
- [37] T. Still, M. Mattarelli, D. Kiefer, G. Fytas, and M. Montagna, *J. Phys. Chem. Lett.* **1**, 2440 (2010).
- [38] J. G. Berryman and H. F. Wang, *J. Geophys. Res.* **100**, 24611 (1995).
- [39] J. G. Berryman and H. F. Wang, *Int. J. Rock Mech. Mining Sci.* **37**, 63 (2000).